RMetS
Royal Meteorological Society

Finite departure from convective quasi-equilibrium: periodic cycle and discharge–recharge mechanism

Jun-Ichi Yano[a]* and Robert Plant [b]
[a]*GAME/CNRM, Météo-France and CNRS, 31057 Toulouse Cedex, France*
[b]*Department of Meteorology, University of Reading, Reading, UK*

*Correspondence to: J.-I. Yano, CNRM, Météo-France, 42 ave Coriolis, 31057 Toulouse Cedex, France.
E-mail: jun-ichi.yano@zmaw.de

A simple self-contained theory is proposed for describing the life cycles of convective systems as a discharge–recharge process.

A closed description is derived for the dynamics of an ensemble of convective plumes based on an energy cycle. The system consists of prognostic equations for the cloud work function and the convective kinetic energy. The system can be closed by introducing a functional relationship between the convective kinetic energy and the cloud-base mass flux.

The behaviour of this system is considered under a bulk simplification. Previous cloud-resolving models as well as bulk statistical theories for ensemble convective systems suggest that a plausible relationship would be to assume that the convective kinetic energy is linearly proportional to the cloud-base mass flux.

As a result, the system reduces to a nonlinear dynamical system with two dependent variables, the cloud-base mass flux and the cloud work function. The fully nonlinear solution of this system always represents a periodic cycle regardless of the initial condition under constant large-scale forcing. Importantly, the inclusion of energy dissipation in this model does not in itself lead the system into equilibrium.

Received 19 March 2011; Revised 26 September 2011; Accepted 28 September 2011; Published online in Wiley Online Library 23 November 2011

Citation: Yano J-I, Plant R. 2012. Finite departure from convective quasi-equilibrium: periodic cycle and discharge–recharge mechanism. *Q. J. R. Meteorol. Soc.* **138**: 626–637. DOI:10.1002/qj.957

1. Introduction

Convective cloud systems in the atmosphere undergo life cycles and it is physically intuitive to consider that a convective system follows a cycle of discharge and recharge. Once a convective event is over ('discharge'), the atmosphere has been stabilized against further moist convection and a break period follows ('recharge'). This break period continues until sufficient potential energy is 'recharged'. Once the potential energy has reached a threshold, convection is triggered and the accumulated potential energy is again 'discharged' as a result. To the best of our knowledge, the terminology 'discharge–recharge' was originally introduced by Bladé and Hartmann (1993) in order to interpret their experiments of tropical instraseaonal variability with a simple nonlinear model. The present article, in turn, interprets this concept more generally for describing the life cycle of any convective system of any scale.

Although this discharge–recharge mechanism has been invoked in the consideration of various tropical convection problems, especially for the Madden–Julian oscillation (MJO: Benedict and Randall, 2007; Thayer–Calder and Randall, 2009), no self-contained theory has been proposed. The purpose of the present article is to present a simple self-contained theory suitable for describing convective discharge–recharge processes.

Our findings stem from our investigations of the time evolution of ensemble convective systems as described by a mass-flux convection parametrization. The mass-flux convection parametrization problem, as originally formulated by Arakawa and Schubert (1974), is followed by the majority of current operational parametrizations (e.g., Tietdke, 1989; Emanuel, 1991; Bechtold *et al.*, 2001). In spite of the theoretical nature of the present study, it therefore contains serious implications for improving mass-flux convection parametrization.

The Arakawa and Schubert (1974) system is well defined in its formulation in so far as dependent physical variables (e.g., moist static energy, total water) are conserved along a parcel movement. Unfortunately, once explicit microphysical processes become an issue the conservation law breaks down and the problem is no longer well-formulated. Extra complications arise due to the need to introduce an explicit description of the convective vertical velocity, as emphasized by Donner (1993).

However, in so far as only conserved variables are considered, there are only two problems to be resolved in order to make the formulation complete. The first problem is the determination of a rule for specifying entrainment and detrainment rates. There have been extensive debates on this issue (Raymond and Blyth, 1986; Blyth, 1993) which persist to this day (cf., Yano and Bechtold, 2009). The second problem, called 'closure', is to define the mass flux at cloud base. As emphasized by Arakawa and Schubert (1974), 'The real conceptual difficulty in parameterizing cumulus convection starts from this point'. Although extensive progress has been made since that time (Arakawa and Chen, 1987; Xu, 1994), the statement is still valid even today (Arakawa, 2004; Yano *et al.*, 2005a).

In order to address the closure problem, Arakawa and Schubert (1974) pursued the idea of constructing an energy cycle for a convective system. In Arakawa and Schubert's point of view, this cycle is chiefly described by two equations. The first is the budget equation for convective kinetic energy, as given by their eq. (132). This equation shows that the rate of generation of convective kinetic energy is proportional to a quantity named the 'cloud work function' by Arakawa and Schubert. Thus, they proposed also to use the tendency equation for the cloud work function as the second equation of this pair, as given by their eq. (142). The latter equation shows that the cloud work function is consumed at a rate proportional to the cloud-base mass flux.

Arakawa and Schubert closed the problem by seeking a steady solution to the cloud work-function equation, assuming a balance between cloud work-function generation by large-scale forcing and consumption by convection. Such a condition is called *convective quasi-equilibrium*. Mathematically speaking, the problem reduces to that of matrix inversion to find a solution of the cloud-base mass flux. It turns out that this matrix inversion problem is not straightforward in practice, and various approaches have been proposed (Lord, 1982; Lord *et al.*, 1982; Hack *et al.*, 1984; Moorthi and Suarez, 1992).

Randall and Pan (1993) and Pan and Randall (1998) recognized that the problem can more easily be closed in a prognostic manner. Note that the pair equation system considered by Arakawa and Schubert (1974: their eqs (132) and (142)) contains three dependent variables: convective kinetic energy, cloud work function and cloud-base mass flux. It seems reasonable to expect that there is a certain functional relationship between the convective kinetic energy and the cloud-base mass flux. More specifically, those authors assumed the convective kinetic energy to be proportional to the square of the cloud-base mass flux.

In the present article, we note that this functional relationship can be generalized by assuming a power-law dependence of convective kinetic energy on cloud-base mass flux. After reviewing cloud-resolving modelling (CRM) as well as statistical theories, we propose an alternative assumption that the convective kinetic energy is proportional to the cloud-base mass flux. The goal of the present article is to investigate the basic behaviour of the resulting energy-cycle description of convective systems under a bulk simplification (cf., Yanai *et al.*, 1973; Plant, 2010), i.e., in the case in which only one convective mode is assumed. Recall that a continuous spectrum of convective plumes is considered in Arakawa and Schubert (1974). As it turns out, this nonlinear system produces a periodic cycle with a process of discharge and recharge.

The article is organized as follows: the formulation of the problem is presented in the next section, which also includes a review of relevant CRM and theoretical studies. The derived system is investigated in section 3, implications are discussed in section 4 and the article is concluded in section 5.

2. Formulation of the problem

2.1. *Energy cycle of the convective system*

By following the idea of a bulk mass-flux convection parametrization, we consider a system consisting of only a single type of convection. In Arakawa and Schubert's original formulation, this corresponds to the case of a single type of entraining convective plume with a given fractional entrainment rate. However, the problem can be generalized to encompass any other description of a convective plume. In more general cases, the computation of the cloud work-function consumption rate γ, to be introduced later, is more involved than the one given in appendix B of Arakawa and Schubert (1974). Only the order of magnitude of γ is of concern in the present study. A more explicit formulation for general cases is left for future study.

An important aspect of Arakawa and Schubert's mass-flux parametrization is the fact that convection is always considered in terms of an ensemble of plumes, in which there are always a number of convective elements present belonging to each type. What is considered is the evolution of each subensemble, and the evolution of a single convective plume is never a concern. As a result, the triggering of a single convective event, for example, cannot be described under the present formulation: cf., section 3.8.

Here we consider the evolution of an ensemble of convective elements, to be called plumes, under a bulk simplification which assumes that every convective plume in the system can be treated as having the same vertical convective mass-flux profile. We designate the normalized vertical profile as $\eta(z)$, which is a function of height z only. The normalization factor is $m_{\mathrm{B},j}$, the mass flux at cloud base for the given plume, such that the mass flux of a given plume j is

$$m_j = m_{\mathrm{B},j}\eta(z).$$

The total convective mass flux is given by

$$M_c = M_B \eta(z), \tag{1}$$

with the total cloud-base mass flux being given by

$$M_B = \sum_j m_{B,j},$$

with the summation extending over all plumes within the area of interest (e.g., grid box).

In the same manner, the other dependent variables of the problem, the convective kinetic energy K and the cloud work function A, are considered in the present study in terms of the total for all convective plumes. In other words, only the evolution of an ensemble of plumes of a single type is considered, and no attention is paid to the evolution of individual plumes. Note that, by definition, the total cloud-base mass flux M_B is a function of time only.

The evolution of convective kinetic energy consists of a competition between the generation rate G from the buoyancy force and the dissipation D:

$$\frac{dK}{dt} = G - D. \tag{2}$$

Here,

$$G = \int_{z_B}^{z_T} M_c b \, dz, \tag{3}$$

with the integral extending from cloud base z_B to cloud top z_T and b being the buoyancy, defined in the case of Arakawa and Schubert (1974) by

$$b = \frac{g}{C_p \bar{T}}(s_{vc} - \bar{s}_v)$$

in terms of the acceleration due to gravity g, the heat capacity at constant pressure C_p, the temperature T and the virtual static energy $s_v = C_p T_v + gz$, which is defined from the virtual temperature T_v. The overbar and the subscript c designate the area mean and convective components, respectively.

By substituting Eq. (1) into Eq. (3), the kinetic-energy generation rate becomes

$$G = A M_B \tag{4}$$

with the cloud work function defined by

$$A = \int_{z_B}^{z_T} \eta b \, dz. \tag{5}$$

Substitution of Eq. (4) into Eq. (2) then leads to

$$\frac{dK}{dt} = A M_B - D, \tag{6}$$

which is equivalent to eq. (132) of Arakawa and Schubert (1974) under the bulk simplification.

The prognostic equation for the cloud work function is obtained directly, by taking a time derivative of its defining equation, Eq. (5). After lengthy calculations, as outlined in appendix B of Arakawa and Schubert (1974), one can obtain an equation of the form

$$\frac{dA}{dt} = -\gamma M_B + F, \tag{7}$$

which is equivalent to eq. (142) of Arakawa and Schubert (1974), again under the bulk simplification. Note that the factor γ corresponds to a diagonal element of the integral kernel $K(\lambda, \lambda')$ defined in Arakawa and Schubert. We have changed the notation in order to avoid any confusion with the convective kinetic energy K and have also flipped the sign, expecting the first term on the right-hand side of Eq. (7) to be negative in general due to convective damping (see below). A time-independent large-scale forcing F will be assumed in the present study.

Eqs (6) and (7) provide a qualitative description of the evolution of a bulk convective ensemble: large-scale forcing generates the cloud work function with time by Eq. (7). The cloud work function, in turn, generates more convective activity through Eq. (6). This enhancement of convection is associated with an increase of cloud-base mass flux, which in turn damps the cloud work function with time through the first term on the right-hand side of Eq. (7). By physical intuition, therefore, γ should be positive because convection grows by consuming the cloud work function. This notion is called 'convective damping' by Emanuel *et al.* (1994).

A further intuition invoked by Arakawa and Schubert (1974) is that within a relatively short time the rate of consumption of the cloud work function comes into balance with the generation rate by large-scale forcing, and thus we obtain

$$-\gamma M_B + F = 0, \tag{8}$$

which is the state of convective quasi-equilibrium.

The main goal of the present study is to examine the behaviour of the system under *finite departure* from convective quasi-equilibrium by explicitly integrating the pair system, Eqs (6) and (7). According to the original argument by Arakawa and Schubert (1974), summarized above, we would expect that the system approaches equilibrium with time. In order to close this system, a certain functional relationship must be introduced between the convective kinetic energy and the cloud-base mass flux. This issue is considered next.

2.2. *Functional relationship assumption*

We will assume a functional relationship of the form

$$K \propto M_B^p \tag{9}$$

between the convective kinetic energy K and the cloud-base mass flux M_B. Here, p is an unspecified positive constant. In the present article, we will use Eq. (9) with $p = 1$ in order to close the problem. This choice is made based on the following discussions. However, note that various assumptions introduced in course of these discussions should not be considered as crucial for the present model formulation. The choice of any value for p must be regarded as somewhat arbitrary given our current state of knowledge and ultimately the extent of the support for any functional relationship between K and M_B can only be fully established from extensive CRM analyses.

First of all, we must recognize that dimensional analysis between K and M_B does not give a unique answer to the power p. In other words, we cannot make the proportionality constant dimensionless, regardless of the way we choose the power p. In this respect, p remains an arbitrary constant of the problem. Eq. (9) may be considered as a generalized similarity theory between K and M_B, which may be determined by observations or modelling, as we attempt in the subsequent subsections. Nonetheless, the following considerations suggest that $p = 1$ and $p = 2$ are choices of particular physical interest.

Recall that the cloud-base mass flux is more precisely defined by

$$M_B = \rho_B \sigma_B w_B, \tag{10}$$

where ρ is the density, σ the fractional area occupied by convective plumes and w the convective vertical velocity. The subscript B indicates cloud-base values. Similarly, the convective kinetic energy may be defined by

$$K = \int_{z_B}^{z_T} \sigma \frac{\rho}{2} w^2 \, dz. \tag{11}$$

A precise assumption of the form of the convective kinetic energy is not given in Arakawa and Schubert (1974), but for now let us assume, solely for the sake of convenience, that the convective kinetic energy only includes the vertical velocity. A restriction of K to the vertical component makes its link with the cloud-base mass flux more direct, and all the discussions in section 2.3 (together with the evidence from Emanuel and Bister (1996) in section 2.4) are valid with or without this restriction.

We should stress that the restriction of our definition of convective kinetic energy to the vertical component is fully self-consistent regardless of whether the horizontal component of kinetic energy is negligible or not. For example, the simulations of Xu *et al.* (1992) and Xu (1993) suggest that the horizontal component of eddy kinetic energy is an order of magnitude larger than the vertical component. However, this does not necessarily oblige us to include the horizontal component in the definition of K.

A simple energy integral analysis shows that the term proportional to the cloud work function generates the vertical component of convective kinetic energy more directly, as is carefully discussed in Yano *et al.* (2005b). The horizontal component is generated only indirectly by conversion from the vertical component via pressure forcing (Khairoutdinov and Randall, 2002). When the horizontal component is neglected, we can choose to include the conversion rate of the vertical component into the horizontal component as a part of an energy dissipation rate, D. This interpretation is legitimate because vertical kinetic energy is lost in lieu of horizontal kinetic energy.

Alternatively, when the horizontal component is included in the definition of convective kinetic energy, the following analysis can still be reproduced simply by assuming that the horizontal component is always proportional to the vertical component.* It should also be emphasized that the following short analysis is merely for the sake of obtaining a feeling about a possible choice for the exponent p. The functional relationship of Eq. (9) can be introduced without requiring an explicit definition for K. That will be the point of view adopted throughout the remainder of the article. However, let us now proceed to consider the implications of taking the definition of Eq. (11).

By taking an anelastic approximation, we may assume that the density ρ is a function of height only. On the other hand, both σ and w will depend on both time and height. We may separate the dependences by writing these two variables as

$$\sigma = \sigma_B(t)\hat{\sigma}(z), \tag{12a}$$

$$w = w_B(t)\hat{w}(z). \tag{12b}$$

Substitution of Eqs (12a) and (12b) into Eq. (11) leads to

$$K = \sigma_B w_B^2 \hat{K}, \tag{13}$$

where $\hat{K}$ is a constant, independent of time.

Further substitution of Eqs (10) and (13) into Eq. (9) leads to a relation

$$\sigma_B^{p-1} w_B^{p-2} \sim \text{const.}$$

This relationship indicates that the actual power p is dependent on the relative 'strength' of the time dependence of σ_B and w_B.

Cases of particular interest arise from assuming either σ_B or w_B alone to control the time dependence. Arguably the more intuitive case is to assume that only w_B is time-dependent and σ_B is totally time-independent, so that $p = 2$. This is the case considered by Randall and Pan (1993) and Pan and Randall (1998). For constant large-scale forcing, that system leads to a damped harmonic oscillator, although we note that Davies *et al.* (2009) found more complex behaviour for a rapidly varying on/off forcing. An alternative possibility is to assume that only σ_B depends on time and that the cloud-base convective vertical velocity w_B is independent of time. In this case we have $p = 1$, the choice that we investigate in the present article.

2.3. *Equilibrium solution*

In section 2.4 we will review the extent of support for the two possibilities $p = 1$ or 2 from both CRM results and statistical theories. As a prerequisite, we first derive the equilibrium solution under the general similarity relation of Eq. (9) and then examine the expected consequences when $p = 1$ and 2. Note that the discussion of this subject is solely based on seeking a steady solution for the system of Eqs (6) and (7), without invoking any of the further assumptions introduced in the latter part of the previous subsection.

The equilibrium solution M_0 for cloud-base mass flux is obtained directly by solving Eq. (8) under stationary conditions:

$$M_0 = \frac{F}{\gamma}. \tag{14}$$

Thus, the equilibrium cloud-base mass flux should increase linearly with increasing large-scale forcing, regardless of the value of p.

*Table 3 of Khairoutdinov and Randall (2002) would provide some support for such an assumption, at least in a time-mean sense.

The equilibrium solution for the cloud work function is obtained by solving the steady problem for Eq. (6):

$$A_0 = \frac{D}{M_0}.$$

In order to arrive at a closed expression, we need a specific form for the energy dissipation rate, for which we follow Lord and Arakawa (1980) and others by assuming a relaxation

$$D = \frac{K}{\tau_D}, \tag{15}$$

where τ_D is a constant dissipation time-scale. It may be emphasized that this is hardly a unique choice for the energy dissipation rate but is introduced merely as the simplest case. An alternative form for the convective kinetic energy dissipation would be $D \sim K^{2/3}$, as is typically assumed in boundary-layer turbulence theories (cf., Grant and Brown, 1999). Another alternative would be $D \sim M_B$ as suggested[†] by Arakawa (1993) and Arakawa and Cheng (1993).

Substitution of Eqs (9) and (15) into the equilibrium solution for A above leads to

$$A_0 \propto M_0^{p-1}. \tag{16}$$

Thus, if $p = 2$, $A_0 \propto M_0 \propto F$ and the cloud work function increases linearly with increasing large-scale forcing. On the other hand, if $p = 1$, we see that the cloud work function at equilibrium becomes independent of the cloud-base mass flux and hence also independent of large-scale forcing.

These contrasting results are tested against CRM results given in the literature. In the comparison, we focus our attention on idealized CRM experiments under constant large-scale forcing and especially on studies in which the strength of the forcing is varied across otherwise similar experiments. By restricting our attention to a particular class of experiments, the equilibrium solution obtained in the present subsection can be unambiguously compared with 'true' CRM equilibrium solutions. In order to consider a finite departure from quasi-equilibrium in the subsequent analysis, agreement with the dependences at equilibrium is deemed to be a necessary pre-condition. Our focus is further restricted to simulations without background shear flow in order to avoid the influence of mesoscale organization, which the present model does not take into account.

2.4. *Evidence from cloud-resolving modelling*

Various results from CRM studies support the choice $p = 1$ rather than $p = 2$. The first piece of evidence is from figure 2 of Emanuel and Bister (1996). This result from a CRM simulation (dashed curve) shows that CAPE (convective available potential energy: the non-entraining limit of the cloud work function) is approximately invariant with the large-scale forcing, being consistent with the scaling $p = 1$.

Another item of evidence is from figure 8 of Parodi and Emanuel (2009). That figure shows the dependence of the convective updraught velocity on the prescribed precipitating terminal velocity. This dependence itself is not our interest here. However, an important point is that the curve for the convective updraught velocity does not change much by changing the prescribed radiative cooling rate (large-scale forcing) from 2 K day^{-1} to 6 K day^{-1}.

Table 1 of Shutts and Gray (1999), obtained from their CRM experiments, also shows that the convective vertical velocity is approximately invariant with large-scale forcing. The statistical theories of both Emanuel and Bister (1996) and Shutts and Gray (1999) also make this prediction. These results suggest therefore that the convective vertical velocity is rather invariant and so it is the fractional area of convection that increases with increasing large-scale forcing, being consistent with the choice $p = 1$ if either the convective kinetic energy is restricted to the vertical component or the horizontal component can be assumed to be proportional to the vertical component.

A major exception in the literature pointing to $p = 2$ is Xu (1993). However, the evidence shown by his figure 22.15 supports this Ansatz only for an active phase of convection. A more serious problem with quoting the result is that, as is clearly emphasized in the original article, the mesoscale convective organization dominates the eddy 'convective' kinetic energy defined therein, whereas here we consider the situation without mesoscale organization.

Another piece of unfavourable evidence is found in figure 4 of Jones and Randall (2011). This shows that the cloud fraction is rather invariant with a change of large-scale forcing in their constant-forcing experiments. This clearly favours $p = 2$ rather than $p = 1$ according to the analysis of the equation immediately after Eq. (13). However, caution is required in interpreting that result for the present context, as Jones and Randall (2011) were concerned with the total cloud fraction as defined through a condensate threshold rather than the convective cloud fraction directly associated with updraught cores, which is the concern here.

Taken as a whole, we consider that the evidence supporting $p = 1$ is strongly suggestive but hardly overwhelming. Perhaps surprisingly, the number of CRM studies comparing the convection produced by different strengths of constant large-scale forcing is rather limited. Further investigation is clearly required. Moreover, any investigation into the equilibrium state of potential energy convertibility (PEC), a CRM equivalent to the cloud work function (Yano *et al.*, 2005b), instead of CAPE is yet to be performed to the best of our knowledge. Nevertheless, the use of a simple proportionality hypothesis $p = 1$ in the functional relationship of Eq. (9) appears to be a very reasonable possibility to consider, and no analysis published so far excludes this possibility in any clear sense.

3. Analysis

3.1. *Governing equation system*

Based on the review of CRM results in the previous subsection, we now set $p = 1$ in Eq. (9):

$$K = \beta M_B, \tag{17}$$

where the time-independent constant β is defined by

$$\beta = w_B \int_{z_B}^{z_T} \left(\frac{\rho_B}{\rho}\right) \frac{\eta^2}{2\hat{\sigma}}\, dz. \tag{18}$$

[†]Apparently on the basis that it leads to an equilibrium value of the cloud work function that is independent of forcing strength, a property that would hold regardless of the value of p.

By substituting Eqs (15) and (17) into Eqs (6) and (7), we finally obtain a closed governing equation system:

$$\frac{\mathrm{d}M_\mathrm{B}}{\mathrm{d}t} = \frac{M_\mathrm{B}}{\tau_\mathrm{D}}\left(\frac{A-A_0}{A_0}\right), \tag{19a}$$

$$\frac{\mathrm{d}A}{\mathrm{d}t} = -\gamma M_\mathrm{B} + F, \tag{19b}$$

where

$$A_0 = \frac{\beta}{\tau_\mathrm{D}} \tag{20}$$

is the equilibrium solution for the cloud work function. We also recall that the equilibrium solution for the cloud-base mass flux is as given in Eq. (14).

The obtained equation system is nonlinear due to the product of A and M_B appearing on the right-hand side of Eq. (19a), i.e., the generation rate of cloud-base mass flux increases nonlinearly with increasing strength of convection. This nonlinearity leads to the discharge–recharge mechanism shown below.

3.2. Non-dimensionalization

In order to analyze the system (19) it is convenient first to non-dimensionalize it by setting

$$M_\mathrm{B} = M_0(1+x), \tag{21a}$$

$$A = A_0(1+y), \tag{21b}$$

and also to non-dimensionalize the time t by τ_D. We also designate the time derivative by a dot in the following for economy of presentation.

As a result, the non-dimensionalized governing equations read

$$\dot{x} = (1+x)y, \tag{22a}$$

$$\dot{y} = -\tilde{f}x. \tag{22b}$$

Here,

$$\tilde{f} = \frac{F}{\beta}\tau_\mathrm{D}^2 \tag{23a}$$

is the non-dimensionalized large-scale forcing and the sole non-dimensional parameter of the problem.

Indeed, with a slightly more subtle rescaling we can further absorb this non-dimensional parameter, and so write down universal equations independent of $\tilde{f}$. Thus, we non-dimensionalize the cloud work function by setting

$$A = A_0(1+\tilde{f}^{1/2}y) \tag{23b}$$

in place of Eq. (21b) and taking $\tilde{f}^{-1/2}\tau_\mathrm{D}$ as a time-scale for non-dimensionalization in place of τ_D. As result, Eqs (22a) and (22b) are transformed into the universal form:

$$\dot{x} = (1+x)y, \tag{24a}$$

$$\dot{y} = -x. \tag{24b}$$

The renormalization of Eq. (23b) reveals that relative fluctuations, $(A-A_0)/A_0$, of the cloud work function scale with $\tilde{f}^{1/2}$, i.e., they increase with increasing non-dimensional forcing.

3.3. Estimate of parameters

After the rescaling of the previous subsection, the solution becomes universal independent of the physical parameters of the problem. Nonetheless, in order to establish the context, before we proceed with the rescaled system, we provide some estimates of typical values of the physical parameters.

A typical value for β, defined by Eq. (18), is estimated as

$$\beta \sim Hw_\mathrm{B} \sim 10^4\,\mathrm{m} \times 1\,\mathrm{m\,s^{-1}} \sim 10^4\,\mathrm{m^2\,s^{-1}},$$

with $H \sim 10^4$ m the tropospheric depth and $w_\mathrm{B} \sim 1\,\mathrm{m\,s^{-1}}$. Here we have assumed the integrand to be of order unity. In practice, explicit evaluation of the integral using a simple entraining plume model for deep convection in a typical tropical sounding produced $\int_{z_\mathrm{B}}^{z_\mathrm{T}}(\rho_\mathrm{B}/\rho)^2\eta\,\mathrm{d}z \simeq 6H$ and we may set $\hat{\sigma} \simeq 1$. Thus, the above estimate seems likely to be an underestimate by a factor of a few.

The large-scale forcing F is defined by eq. (B33) in Arakawa and Schubert (1974). A simple scale analysis suggests that the dominant contribution to the large-scale forcing comes from the large-scale (LS) tendency $(\partial\bar{s}_\mathrm{v}/\partial t)_\mathrm{LS}$ of the virtual static energy. This contribution can furthermore be approximated from the large-scale tendency of potential temperature θ, which mainly consists of the large-scale ascent $-\bar{w}(\partial\bar{\theta}/\partial z)$ and the radiative heating Q_R. Both of these terms have a comparable magnitude and are of order $3\,\mathrm{K\,day^{-1}}$ in total. Thus, the large-scale forcing is approximately given by

$$F \simeq -\int_{z_\mathrm{B}}^{z_\mathrm{T}} g\frac{\eta}{C_\mathrm{p}\bar{T}}\left(\frac{\partial\bar{s}_\mathrm{v}}{\partial t}\right)_\mathrm{LS}\mathrm{d}z \simeq \int_{z_\mathrm{B}}^{z_\mathrm{T}} g\frac{\eta}{\bar{T}}\left(\bar{w}\frac{\partial\bar{\theta}}{\partial z} - Q_\mathrm{R}\right)\mathrm{d}z.$$

This then leads to the estimate

$$\begin{aligned} F &\sim \frac{Hg}{T_0}|Q_\mathrm{R}| \\ &\sim 10^4\,\mathrm{m} \times 10\,\mathrm{m\,s^{-2}} \times (300\,\mathrm{K})^{-1} \times 3 \times 10^{-5}\,\mathrm{K\,s^{-1}} \\ &\sim 10^{-2}\,\mathrm{J\,kg^{-1}\,s^{-1}}. \end{aligned}$$

Here $T_0 \sim 300$ K is the surface temperature and 1 day $\sim 10^5$ s.

Note that the above estimate of the large-scale forcing can be considered a median value for the wide range of values possible. The large-scale forcing may be much larger under strong large-scale ascent or much weaker (even negative) under large-scale descent.

An estimation of the convective damping rate γ can be obtained from eqs (B36) and (B37) of Arakawa and Schubert (1974). It can be shown that so long as the precipitation efficiency of convection is close to unity the dominant damping term is adiabatic warming due to the environmental compensating descent (cf., figure 11 of Arakawa and Schubert, 1974), which is approximately given by

$$\begin{aligned} \gamma &\simeq \int_{z_\mathrm{B}}^{z_\mathrm{T}} g\frac{\eta^2}{\rho C_\mathrm{p}\bar{T}}\frac{\partial\bar{s}_\mathrm{v}}{\partial z}\,\mathrm{d}z \\ &\simeq \int_{z_\mathrm{B}}^{z_\mathrm{T}} g\frac{\eta^2}{\rho\bar{T}}\frac{\partial\bar{\theta}}{\partial z}\,\mathrm{d}z \sim g\frac{H}{\rho_\mathrm{B}T_0}\frac{\partial\bar{\theta}}{\partial z} \\ &\sim 10\,\mathrm{m\,s^{-2}} \times \frac{10^4\,\mathrm{m}}{1\,\mathrm{kg\,m^{-3}} \times 300\,\mathrm{K}} \times 3 \times 10^{-3}\,\mathrm{K\,m^{-1}} \\ &\sim 1\,\mathrm{J\,m^2\,kg^{-2}}. \end{aligned}$$

An explicit evaluation of the actual integral produced $\int_{z_B}^{z_T} \eta^2/\rho \, dz \simeq 2H$. The factor of 2 was neglected in the above estimate.

As a consequence of the above estimates, a typical equilibrium mass flux is estimated to be

$$M_0 = \frac{F}{\gamma} \sim 10^{-2}\,\mathrm{kg\,m^{-2}\,s^{-1}}.$$

A suitable estimate for the kinetic energy dissipation time-scale τ_D is less clear. The suggestion of Randall and Pan (1993) and Pan and Randall (1998) was that $\tau_D \sim 10^3$ s, while Khairoutdinov and Randall (2002) computed values in the range 4–8 h for the dissipation of a kinetic energy measure that included contributions from the horizontal components of velocity and mesoscale eddies. On the other hand, if we suppose that the dissipation rate is primarily controlled by the convective entrainment rate, as suggested by de Roode *et al.* (2000), then we obtain

$$\tau_D \sim \frac{\sigma \rho_B}{\lambda M_0} \sim 10^5\,\mathrm{s} \sim 1\,\mathrm{day}$$

for $\sigma \sim 10^{-1}$, $\rho_B \sim 1\,\mathrm{kg\,m^{-3}}$, a fractional entrainment rate $\lambda \sim 10^{-4}\,\mathrm{m^{-1}}$ and $M_0 \sim 10^{-2}\,\mathrm{kg\,m^{-2}\,s^{-1}}$. This is rather a long time-scale.

As a result, the equilibrium cloud work function is estimated to be in the range

$$A_0 = \frac{\beta}{\tau_D} \sim 10^{-1}\text{–}10\,\mathrm{J\,kg^{-1}}.$$

Such values are smaller than typically observed values for CAPE ($\sim 10^3\,\mathrm{J\,kg^{-1}}$) but are not too dissimilar to observational estimates of the cloud work function for relatively low clouds (with cloud-top heights of less than ~ 300 hPa), as given by figures 9–11 of Lord and Arakawa (1980). Broadly similar values, much smaller than CAPE, have typically been quoted for generalized CAPE (Wang and Randall, 1994; Xu and Randall, 1998). Recall also that β is rather underestimated here.

Finally, by putting all of these estimates together, the non-dimensional forcing parameter is estimated to be in the range

$$\tilde{f} = \frac{F\tau_D^2}{\beta} \sim 1\text{–}10^4.$$

Note that this is an upper-bound estimate, because β could be larger and the large-scale forcing could be weaker under a descending environment.

3.4. Perturbation analysis

The governing system of Eqs (24a) and (24b) is nonlinear. However a perturbation analysis around the equilibrium solution $(x, y) = (0, 0)$ provides some hints about its general behaviour. Linearization of Eqs (24a) and (24b) leads to

$$\dot{x} = y,$$
$$\dot{y} = -x,$$

which furthermore reduces to a single equation for x:

$$\ddot{x} + x = 0.$$

The solution is a sinusoidal oscillation with unit frequency. The corresponding dimensional period is given by $2\pi\tau_D\tilde{f}^{-1/2} = 2\pi(\beta/F)^{1/2}$. By substituting the parameter estimates from the last subsection, a typical period is estimated to be $\sim 6 \times 10^3$ s$\sim$2 h. Note that the period is longer for weaker forcing F and stronger convection β. We expect that the actual period may vary by an order of magnitude around this estimate, depending on the specific case. Most importantly, though, the period is independent of the kinetic-energy dissipation time-scale τ_D.

3.5. Nonlinear periodic orbit

Even in the fully nonlinear regime, it is straightforward to define the orbits of the present system. Eqs (24a) and (24b) can be rewritten as

$$\frac{dx}{(1+x)y} = -\frac{dy}{x} = dt.$$

From the first equality, we obtain

$$\frac{x\,dx}{(1+x)} + y\,dy = 0.$$

Since the two terms depend only on x and y respectively, the above equation is integrable and we obtain the solution

$$x - \ln(1+x) + \frac{y^2}{2} = C, \tag{25}$$

where C is a constant.

It is straightforward to prove that $X(x) \equiv x - \ln(1+x)$ is always positive and thus the above solution (25) constitutes a closed orbit. It also follows that, even in the fully nonlinear regime, the system presents a periodic cycle.

Examination of the form of the function $X(x)$ provides some insight into the shape of the solution orbit. Its Taylor expansion is

$$X(x) = \sum_{n=2}^{\infty} (-1)^n \frac{x^n}{n} = \frac{x^2}{2} - \frac{x^3}{3} + \cdots$$

The most obvious conclusion is that in the small-amplitude limit of $|x| \ll 1$ the orbit is asymptotic to a circle in the (x, y) plane, in agreement with the previous subsection. More importantly, due to the contribution from the cubic term in the expansion, the orbit exhibits an asymmetry between positive and negative x, with $X(x)$ increasing more rapidly for negative x when x moves away from the origin. Consequently, the system must respond to changes in the renormalized cloud work function y by producing weaker changes in x on the negative side (when convective is subdued) than on the positive side (when convection is active).

It is this tendency that leads to the discharge–recharge mechanism that will be shown graphically in the next subsection. In the recovering (recharge) phase with negative x, the convective mass flux x changes only weakly with increasing cloud work function y. On the other hand, once convection is triggered (discharge phase) the enhanced mass flux ($x > 0$) makes a swing of growth and decay by following the decreasing cloud work function y.

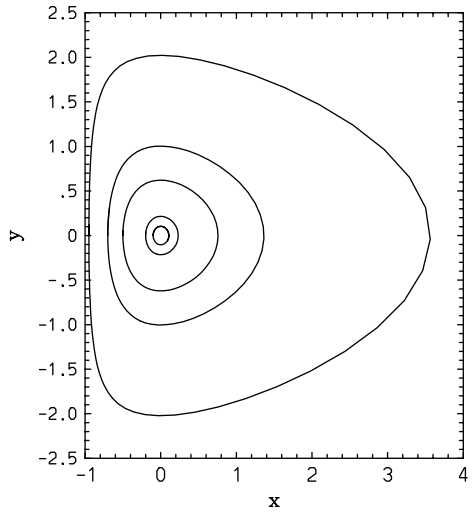

Figure 1. Examples of the solutions in phase space for the simple model (Eqs (24a) and (24b)) representing the convective discharge–recharge process. The x and y axes are the non-dimensionalized mass flux and cloud work function respectively. Five solutions are shown with different initial conditions. All solutions evolve in a clockwise manner, following a cycle of discharge with decreasing cloud work function y and recharge with increasing cloud work function y.

3.6. *Examples of nonlinear solutions*

A full solution for the time evolution of the system of Eqs (24a) and (24b) can be expressed in terms of an elliptic function. However, we do not pursue that path here because a closed expression for the elliptic function is not readily available. Instead, the following results have been produced from numerical time integrations, although, for example, the orbits shown in Figure 1 could also have been plotted directly from Eq. (25).

Example solutions are shown in Figure 1. Numerical time integration is performed with the fourth-order Runge–Kutta method. The figure shows the evolution of the system in phase space, initialized with $y = 0$ and various values for $x(< 0)$. Note that all the solutions evolve in a clockwise manner and recall that $x = -1$ corresponds to zero mass flux (cf., Eq. (21a)), whilst $y = 0$ is the equilibrium value of the cloud work function.

A process for discharge and recharge is noticeable for all of the solutions shown. Initially the cloud work function y simply increases with time by constant forcing with little change in the convection (i.e., $x \sim$ constant). Once the cloud work function reaches a threshold, convection suddenly begins to increase in strength, rapidly consuming the cloud work function. This marks the beginning of the discharge process. Convective mass flux increases until the cloud work function reduces to its equilibrium value ($y = 0$) and thereafter the convective activity reduces towards the initial minimum level while the cloud work function continues to decrease. This marks the beginning of another recharge process: the cloud work function gradually begins to recover in order to prepare for another convectively active phase.

3.7. *Mechanism of discharge–recharge process*

The discharge–recharge of the system stems from the nonlinearity in the generation rate of the cloud work function found on the right-hand side of Eq. (19a). This leads to an asymmetry in the orbit shape (Eq. (25)).

To consider this asymmetry further, it is instructive to perform a perturbation analysis of the system initialized with a state that has near-zero convective activity:

$$x = -1 + \epsilon\zeta,$$

where ζ is a new variable representing the mass flux and the small parameter ϵ measures the closeness of the initial condition to the zero mass-flux state (we may set $\zeta = 1$ as an initial condition). Substitution of the above into Eqs (24a) and (24b) leads to

$$\dot{\zeta} = y\zeta, \tag{26a}$$

$$\dot{y} = 1. \tag{26b}$$

Eq. (26b) shows that the cloud work function increases linearly with time, $y = t$, as a recharge process. Substitution of this result into Eq. (26a) shows that the evolution of mass flux is exponential, $\zeta = \mathrm{e}^{t^2/2}$, with its enhancement becoming noticeable only after a finite time, $t = \mathcal{O}(1)$. This marks the beginning of the discharge process.

In order to demonstrate the recharge–discharge elucidated by the perturbation analysis above, we plot a time series of a solution in Figure 2, using the initial condition $x = -0.95$, $y = 0$. In the initial recharge phase, the cloud work function (long-dashed) increases linearly with time while the mass flux (solid) grows exponentially and only becomes substantial within the following discharge phase. Note that the mass flux (convective activity) as a whole has a pulse-like behaviour, with the clear dichotomy of a quiescent phase (recharge) and an active phase (discharge). The decrease of cloud work function in the discharge phase is slightly faster than the increase in the recharge phase.

3.8. *General features*

As seen from the perturbation analysis in the previous subsection, discharge–recharge is well manifested when the

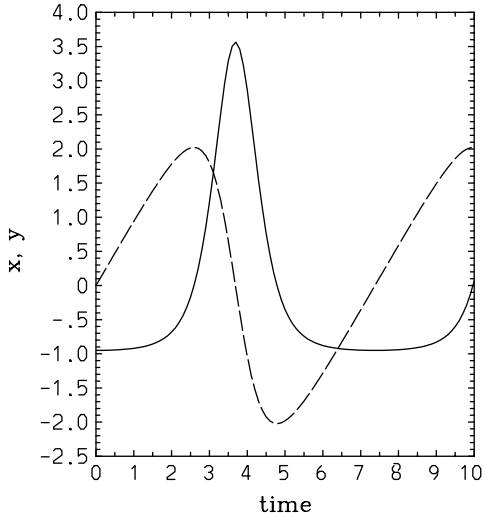

Figure 2. An example time series representing the discharge–recharge process. Enhanced convective activity, measured by the mass flux x (solid line), is triggered only after the cloud work function y (long-dashed line) has been fully recharged. A discharge of convective energy (sudden decrease in both curves) then leads to the next phase of the recharge process. Note that both variables as well as time are given in non-dimensional units. See text for details.

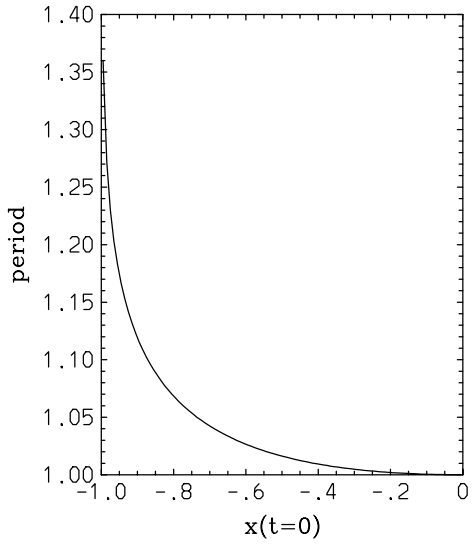

Figure 3. The period of the convective discharge–recharge system as a function of the initial non-dimensional mass flux value $x(t = 0)$. The initial cloud work function is assumed to be at equilibrium (i.e., $y = 0$), and x is defined such that $x = 0$ is the equilibrium state and $x = -1$ corresponds to the state of no convection. Note that the period is normalized by $2\pi(\beta/F)^{1/2}$, as predicted by a perturbation analysis for small x in section 3.4.

initial condition has a small value of mass flux. In this subsection, we turn our attention to some more general features of the system.

A first point to note is that the zero mass-flux state is singular, in the sense that convective activity never develops and so the cloud work function simply continues to increase linearly with time. In other words, a small but finite convective seed is required in order for convection to grow. This reflects the fact that the system only describes the evolution of an ensemble of convection and is incapable of describing the initiation of individual convection, as already emphasized at the beginning of section 2.1.

As the initial condition departs more from zero mass flux (i.e., $x = -1$) and approaches the equilibrium state (i.e., $x = 0$), then discharge–recharge becomes less manifest, as seen in Figure 1. The limit of small x is well described by a linear perturbation around the equilibrium solution, as presented in section 3.4.

The period of the discharge–recharge cycle can, in principle, be evaluated by performing an elliptic integral. Instead, here we prefer a simple numerical approach, defining the period from the time at which y changes sign for the second time (with the initial condition $y = 0$ being used throughout). The result is shown in Figure 3 as a function of the initial mass flux value $x(t = 0)$. Here, the period is scaled such that unity corresponds to the prediction from the perturbation analysis in section 3.4. It is found that the prediction from this linear analysis works quite well for a wide range of initial conditions, except for a tendency towards infinity as the initial condition approaches $x = -1$.

3.9. *Modifications to the model*

The model proposed here is extremely simplified, and thus it is easy to point out various unphysical features and even simply to condemn it as unphysical. At the same time, the model is so simple that it is also extremely easy to try various mathematical variations of the problem, but without firm physical basis. With that general caveat in mind, in this subsection we briefly consider some possible modifications of the model in order to improve its physical relevance.

The most noticeable defect of the present model is a consequence of its prediction that the cloud work function sustains larger variations for larger values of the non-dimensional forcing $\tilde{f}$ and also for smaller values of the initial mass flux (i.e., $x \to -1+$). The model permits such variations to be large enough that the cloud work function can become overdamped, even producing negative values.[‡]

The reason for this defect is our basic premise that the large-scale state is fixed with time. As a result, the convective damping rate γ, which is a function of the environmental state in reality, is treated as a constant in the present formulation. More mathematically, the cloud work function is damped only linearly (Eq. (22b)) and thus there is no possibility of controlling the overdamping tendency. This is in contrast to the mass-flux equation, Eq. (22a), which is controlled by a nonlinear damping that ensures the mass flux always remains positive.

The overdamping of the cloud work function can be prevented by introducing a similar nonlinear damping rate to the cloud work-function equation, rewriting Eq. (22b) as

$$\dot{y} = -\tilde{f}(1 + y)x. \tag{27}$$

Physically, this reformulation is achieved by assuming that both the convective damping rate γ and the large-scale forcing F are proportional to the cloud work function. The latter assumption could be justified by reasoning that large-scale forcing is less effective as the atmosphere approaches neutral stability (i.e., vanishing cloud work function). This assumption leaves the equilibrium solution for the mass flux independent of the cloud work function.

The results after this modification are shown in Figure 4 for the same set of initial conditions as in Figure 1 and for the case with $\tilde{f} = 1$. Note that due to the modification of the system it is no longer possible to transform it into a universal form as for the original system. The modification leads to behaviour still closer to our expectations of discharge–recharge: convective activity continues to increase until the cloud work function is almost depleted and only then does it begin to decay.

A similar modification would be to allow the large-scale forcing to be maintained independently of the value of the cloud work function, while making the convective damping rate γ proportional to the cloud work function as above. In that case, the solution turns into a damping oscillator.

In fact, examination of appendix B of Arakawa and Schubert (1974) shows that the convective damping rate γ is not constant even under a constant environment, but rather it has some explicit dependence on the cloud work function. This stems from the tendency of the mixed-layer height z_B to decrease under a given cloud-base mass flux, as seen in their eq. (B23):

$$\frac{\partial}{\partial t} z_B \sim -\frac{M_B}{\rho_B}.$$

[‡]In fact this is not totally unphysical, but it is clearly against our observational knowledge that the tropical atmosphere is almost always conditionally unstable. A state with a strongly negative CAPE is not observationally known in the tropical atmosphere (cf., Roff and Yano, 2002).

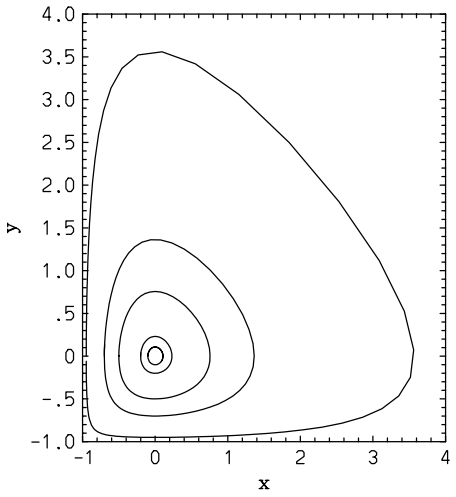

Figure 4. As Figure 1, but with a cloud work-function dependence having been introduced to the cloud work-function tendency equation (cf., Eq. (27)). This additional nonlinearity prevents the cloud work function from overdamping into a negative state ($y < -1$).

According to their eq. (B21), this tendency results in an increasing cloud work function:

$$\frac{\partial}{\partial t}A \sim -\lambda A \frac{\partial}{\partial t} z_{\mathrm{B}} \sim \frac{\lambda}{\rho_{\mathrm{B}}} A M_{\mathrm{B}}.$$

In our notation, this term corresponds to a convective damping rate that depends on the cloud work function as

$$\gamma = \gamma_0 - \frac{\lambda}{\rho_{\mathrm{B}}} A,$$

with γ_0 a constant. Qualitatively speaking, the additional term can be considered as a destabilization tendency of the system due to the boundary-layer forcing.

The same perturbation analysis as in section 3.4 shows that this modification leads to an exponentially growing oscillator. Numerical experiments support this tendency for larger departures from the equilibrium state. However, the growth rate is rather slow and substitution of standard values gives an estimate $\lambda M_0/\rho_{\mathrm{B}} \sim 10^{-6}\ \mathrm{s}^{-1}$ as a growth rate.

Finally, we mention the effect of a modification of the functional relationship of Eq. (9) by setting the power $p = 1 + \mu$. A small positive value for μ is suggested by the CRM results discussed in section 2.4, in the sense that variations in σ_{B} are not completely sufficient to explain the CRM results described. The solution becomes a decaying orbit, with a slow approach towards the equilibrium state being governed by the value of μ. If μ is taken to be small and negative, however, the solution spirals slowly away from the equilibrium state.

4. Discussion

The present article shows that under an idealized, constant, large-scale forcing a convective system under convective damping does not necessarily approach an equilibrium state over time, but rather could remain in a perpetual periodic cycle. A typical period cycle, of the order of hours, identified in the present model is arguably much shorter than the characteristic time-scale, of the order of days, expected for typical large-scale processes. For this reason, the finding does not necessarily contradict the observational evidence for convective quasi-equilibrium (most notably figure 13 of Arakawa and Schubert, 1974, but see also Yano *et al.*, 2000).

However, the persistent, finite departure from equilibrium is potentially relevant for various convective systems, especially because the cycle is longer for weaker large-scale forcing. A first possible application could be as a (partial) explanation for the delay of convective onset in the diurnal cycle (cf., Guichard *et al.*, 2004). In the diurnal cycle, it is commonly believed (*ibid*) that the pre-existence of shallow convection is crucial in order to trigger deep convection. However, a finite departure from quasi-equilibrium could be more fundamental, as emphasized by Jones and Randall (2011). The present model captures the basic behaviour of a convective system under such a finite departure, even though shallow convection is not explicitly considered.

The present model could even be considered as a very crude prototype for the MJO under a discharge–recharge mechanism (Bladé and Hartmann, 1993; Benedict and Randall, 2007; Thayer–Calder and Randall, 2009) with very weak large-scale forcing. The gap in scales that would have to be breached in order to justify such an application is rather large, but may not be totally unreasonable, given that the large-scale forcing can vary from positive to negative over the whole cycle of the MJO and thus the mean large-scale forcing could be rather weak. This interpretation may even not be inconsistent with the 'observed' convective quasi-equilibrium, because the cloud work function (CAPE) is expected to fluctuate only weakly and slowly in the limit of weak forcing. Nevertheless, further study is clearly required by explicitly coupling the present model with a simple large-scale dynamical model.

Some subtle issues of the present model are also remarked upon here.

1. The discharge–recharge process in the present study is a consequence of the special choice $p = 1$ for the similarity-relation parameter in Eq. (9). Note that the case with $p = 2$ considered by Pan and Randall (1998) leads to a damping solution under constant large-scale forcing, with the damping time-scale being given by τ_{D} as inspection of their eq. (30) suggests.
2. No 'triggering' process can be considered under the present formulation in the strict sense: rather, the presence of pre-existing convection is an important precondition in order to see the subsequent enhancement of convection.
3. The present formulation provides a way of predicting the convective-plume population with time under the assumption of a fixed strength for the individual convective plumes. In order to consider also the possible time dependence of this strength, as measured by the cloud-base convective vertical velocity w_{B}, an additional prognostic equation would be required, for which additional assumptions would be needed (cf., Yano *et al.*, 2010).
4. Although the present study makes a bulk simplification, it is straightforward to generalize the formulation to treat a spectrum of convective plumes.

5. Conclusions

We have proposed a simple equation set suitable for studying the time evolution of a convective system. The equations

used are those for the energy cycle of an ensemble of convective plumes, as originally introduced by Arakawa and Schubert (1974). The system is closed by introducing an Ansatz for the functional relationship between the convective kinetic energy and the cloud-base mass flux. Thus, the derivation of our equation set is conceptually similar to that of Randall and Pan (1993) and Pan and Randall (1998). The key difference is in the Ansatz chosen. The earlier authors posited $K \sim M_B^2$ but we have argued that this form is not favoured by the dependences expected from equilibrium statistical theories and the results from various equilibrium CRM studies (Emanuel and Bister, 1996; Shutts and Gray, 1999; Parodi and Emanuel, 2009). In order better to respect those CRM results, we investigate instead the equation set resulting from $K \sim M_B$.

A linear analysis shows that the equilibrium state is neutral, such that any perturbation from the equilibrium state produces a periodic solution. The fully nonlinear analysis shows further that any solution from any initial condition takes the form of a periodic cycle. An exact solution is available in terms of an elliptic function, while the shape of the orbit in phase space can be determined by a simple analytical method. The orbital period depends on the distance of the initial state from the equilibrium state.

Qualitatively, the periodic orbit takes on an approximately 'triangular' form. With the system initialized from a state of low convective kinetic energy and low cloud work function, it gradually evolves towards a high cloud work-function state but without noticeable change of kinetic energy (a recharge process). Once the cloud work function reaches a threshold, convective activity increases rapidly. The kinetic energy increases by following a roughly linear trajectory and this continues until the cloud work function has been reduced to its equilibrium value. From there, the kinetic energy makes a sudden turn and begins to decrease by following a roughly linear trajectory until it reaches a minimum. The orbit has then been closed, the discharge process is over and a new cycle of recharge begins.

The recharge-discharge mechanism is often invoked in the context of the MJO. Note that although the period predicted for the recharge–discharge periodic cycle by the present study is much shorter, a particular regime with much weaker mean large-scale forcing and stronger individual convective elements (i.e., larger β) could help to explain the MJO cycle. The present study also suggests that a consideration of finite departures from the equilibrium state may be important in order to understand the time evolution of various atmospheric convective systems, not only the MJO but also the diurnal cycle of convection, for example.

Further investigations are clearly warranted. For an application to the MJO, coupling of the model with large-scale dynamics is crucial. For an application to the diurnal cycle, the inclusion of shallow convection as a second convective type in the energy-cycle description is the next step to take. At the most fundamental level, more extensive CRM analyses are required[§] in order to define the most plausible exponent value p in the proposed generalized similarity theory of Eq. (9).

The energy cycle of the convective system considered in the present work has much wider applicability. It opens a possible route towards statistical cumulus dynamics, a methodology proposed by Arakawa and Schubert (1974) as a systematic approach to the closure problem. At present, only semi-phenomenological descriptions of some aspects of equilibrium statistical cumulus dynamics exist (e.g., Cohen and Craig, 2004, 2006; Craig and Cohen, 2006; Plant and Craig, 2008; Plant, 2009). In order to address time-varying applications, such investigations should also be compared with suitable CRM analyses of plume statistics, such as those produced by Xu and Randall (2001).

[§]Some suitable diagnostics towards this end were very recently published by Jones and Randall (2011), their figures 9 and 12 showing the evolution of cloudy updraught mass flux and the vertical component of kinetic energy, respectively. Unfortunately for our present purposes the figures were constructed from different simulations and so cannot be used as a direct test for a particular functional relationship between those quantities.

Acknowledgements

Discussions with Till Wagner have helped to inspire the present work. Thanks are also due to Cathy Hohenegger for her careful reading of the manuscript. This work was supported by a joint project award from the Royal Society and CNRS. Discussions through the COST Action ES0905 are also acknowledged.

References

Arakawa A. 1993. Closure assumptions in the cumulus parametrization problem. In *The Representation of Cumulus Convection in Numerical Models*, Emanuel KA, Raymond DJ. (eds.) *Meteorological Monographs* **46**: 1–15. Amer. Meteorol. Soc.: Boston, MA.

Arakawa A. 2004. The cumulus parametrization problem: Past, present, and future. *J. Climate* **17**: 2493–2525.

Arakawa A, Chen J-M. 1987. 'Closure assumptions in the cumulus parametrization problem'. In *Short- and Medium-Range Numerical Weather Prediction: Collection of Papers at the WMO/IUGG NWP Symposium, Tokyo, 4–8 August 1986*, pp 107–131.

Arakawa A, Cheng M-D. 1993. The Arakawa–Schubert cumulus parametrization. In *The Representation of Cumulus Convection in Numerical Models*, Emanuel KA, Raymond DJ. (eds.) *Meteorological Monographs* **46**: 123–136. Amer. Meteorol. Soc.: Boston, MA.

Arakawa A, Schubert WH. 1974. Interaction of a cumulus cloud ensemble with the large-scale environment, Part I. *J. Atmos. Sci.* **31**: 674–701.

Bechtold P, Bazile E, Guichard F, Mascart P, Richard E. 2001. A mass-flux convection scheme for regional and global models. *Q. J. R. Meteorol. Soc.* **127**: 869–889.

Benedict JJ, Randall DA. 2007. Observed characteristics of the MJO relative to maximum rainfall. *J. Atmos. Sci.* **64**: 2332–2354.

Bladé I, Hartmann DL. 1993. Tropical intraseasonal oscillations in a simple nonlinear model. *J. Atmos. Sci.* **50**: 2922–2939.

Blyth AM. 1993. Entrainment in cumulus clouds. *J. Appl. Meteorol.* **32**: 626–641.

Cohen BG, Craig GC. 2004. The response time of a convective cloud ensemble to a change in forcing. *Q. J. R. Meteorol. Soc.* **130**: 933–944.

Cohen BG, Craig GC. 2006. Fluctuations in an equilibrium convective ensemble. Part II: Numerical experiments. *J. Atmos. Sci.* **63**: 2005–2015.

Craig GC, Cohen BG. 2006. Fluctuations in an equilibrium convective ensemble. Part I: Theoretical formulation. *J. Atmos. Sci.* **63**: 1996–2004.

Davies L, Plant RS, Derbyshire SH. 2009. A simple model of convection with memory. *J. Geophys. Res.* **114**: D17202.

de Roode SR, Duynkerke PG, Siebesma AP. 2000. Analogies between mass-flux and Reynolds-averaged equations. *J. Atmos. Sci.* **57**: 1585–1598.

Donner LJ. 1993. A cumulus parametrization including mass fluxes, vertical momentum dynamics, and mesoscale effects. *J. Atmos. Sci.* **50**: 889–906.

Emanuel KA. 1991. A scheme for representing cumulus convection in large-scale models, *J. Atmos. Sci.* **48**: 2313–2335.

Emanuel KA, Bister M. 1996. Moist convective velocity and buoyancy scales. *J. Atmos. Sci.* **53**: 3276–3285.

Emanuel KA, Neelin JD, Bretherton CS. 1994. On large-scale circulations in convecting atmosphere. *Q. J. R. Meteorol. Soc.* **120**: 1111–1143.

Grant ALM, Brown AR. 1999. A similarity hypothesis for cumulus transports. *Q. J. R. Meteorol. Soc.* **133**: 25–36.
Guichard F, Petch JC, Redelsperger JL, Bechtold P, Chaboureau J-P, Cheinet S, Grabowski W, Grenier H, Jones CG, Kohler M, Piriou J-M, Tailleux R, Tomasini M. 2004. Modelling the diurnal cycle of deep precipitating convection over land with cloud-resolving models and single-column models. *Q. J. R. Meteorol. Soc.* **604**: 3139–3172.
Hack JJ, Schubert WH, Silva Dias PL. 1984. A spectral cumulus parametrization for use in numerical models of the tropical atmosphere. *Mon. Weather Rev.* **112**: 704–716.
Jones TR, Randall DA. 2011. Quantifying the limits of convective parametrizations. *J. Geophys. Res.* **116**: D08210.
Khairoutdinov MF, Randall DA. 2002. Similarity of deep continental cumulus convection as revealed by a three-dimensional cloud-resolving model. *J. Atmos. Sci.* **59**: 2550–2566.
Lord SJ. 1982. Interaction of a cumulus cloud ensemble with the large-scale environment. Part III: Semi-prognostic test of the Arakawa–Schubert cumulus parametrization. *J. Atmos. Sci.* **39**: 88–103.
Lord SJ, Arakawa A. 1980. Interaction of a cumulus cloud ensemble with the large-scale environment, Part II. *J. Atmos. Sci.* **37**: 2677–2692.
Lord SJ, Chao WC, Arakawa A. 1982. Interaction of a cumulus cloud ensemble with the large-scale environment. Part IV: The discrete model. *J. Atmos. Sci.* **39**: 104–113.
Moorthi S, Suarez MJ. 1992. Relaxed Arakawa–Schubert. A parametrization of moist convection for general circulation models. *Mon. Weather Rev.* **120**: 978–1002.
Pan D-M, Randall DA. 1998. A cumulus parametrization with prognostic closure, *Q. J. R. Meteorol. Soc.* **124**: 949–981.
Parodi A, Emanuel K. 2009. A theory for buoyancy and velocity scales in deep moist convection. *J. Atmos. Sci.* **66**: 3449–3463.
Plant RS. 2009. Statistical properties of cloud lifecycles in cloud-resolving models. *Atmos. Chem. Phys.* **9**: 2195–2205.
Plant RS. 2010. A review of the theoretical basis for bulk mass flux convective parametrization. *Atmos. Chem. Phys.* **10**: 3529–3544.
Plant RS, Craig GC. 2008. A stochastic parametrization for deep convection based on equilibrium statistics. *J. Atmos. Sci.* **65**: 87–105.
Randall DA, Pan D-M. 1993. Implementation of the Arakawa–Schubert cumulus parametrization with a prognostic closure. In *The Representation of Cumulus Convection in Numerical Models*, Emanuel KA, Raymond DJ. (eds.) *Meteorological Monographs* **46**: 137–144. Amer. Meteorol. Soc.: Boston, MA.
Raymond DJ, Blyth AM. 1986. A stochastic mixing model for nonprecipitating cumulus clouds. *J. Atmos. Sci.* **43**: 2708–2718.
Roff GL, Yano J-I. 2002. Convective variability in the CAPE phase space. *Q. J. R. Meteorol. Soc.* **128**: 2317–2333.
Shutts GJ, Gray MEB. 1999. Numerical simulations of convective equilibrium under prescribed forcing. *Q. J. R. Meteorol. Soc.* **125**: 2767–2787.
Thayer-Calder K, Randall DA. 2009. The role of convective moistening in the Madden–Julian oscillation. *J. Atmos. Sci.* **66**: 3297–3312.
Tiedtke M. 1989. A comprehensive mass flux scheme of cumulus parametrization in large-scale models. *Mon. Weather Rev.* **117**: 1779–1800.
Wang J, Randall DA. 1994. The moist available energy of a conditionally unstable atmosphere. Part II: Further analysis of GATE data. *J. Atmos. Sci.* **51**: 703–710.
Xu K-M. 1993. Cumulus ensemble simulation. In *The Representation of Cumulus Convection in Numerical Models*, Emanuel KA, Raymond DJ. (eds.) *Meteorological Monographs* **46**: 221–235. Amer. Meteorol. Soc.: Boston, MA.
Xu K-M. 1994. A statistical analysis of the dependency of closure assumptions in cumulus parametrization on the horizontal resolution. *J. Atmos. Sci.* **51**: 3674–3691.
Xu K-M, Randall DA. 1998. Influence of large-scale advective cooling and moistening effects on the quasi-equilibrium behaviour of explicitly simulated cumulus ensembles. *J. Atmos. Sci.* **55**: 896–909.
Xu K-M, Randall DA. 2001. Updraft and downdraft statistics of simulated tropical and midlatitude cumulus convection. *J. Atmos. Sci.* **58**: 1630–1649.
Xu K-M, Arakawa A, Krueger SK. 1992. The macroscopic behaviour of cumulus ensembles simulated by a cumulus ensemble model. *J. Atmos. Sci.* **49**: 2402–2420.
Yanai M, Esbensen S, Chu J-H. 1973. Determination of bulk properties of tropical cloud clusters from large-scale heat and moisture budgets. *J. Atmos. Sci.* **30**: 611–627.
Yano J-I, Bechtold P. 2009. Toward physical understanding of cloud entrainment–detrainment process. *EOS* **90**: 258.
Yano J-I, Grabowski WW, Roff GL, Mapes BE. 2000. Asymptotic approaches to convective quasi-equilibrium. *Q. J. R. Meteorol. Soc.* **126**: 1861–1887.
Yano J-I, Redelsperger J-L, Guichard F, Bechtold P. 2005a. Mode decomposition as a methodology for developing convective-scale representations in global models. *Q. J. R. Meteorol. Soc.* **131**: 2313–2336.
Yano J-I, Chaboureau J-P, Guichard F. 2005b. A generalization of CAPE into potential-energy convertibility. *Q. J. R. Meteorol. Soc.* **131**: 861–875.
Yano J-I, Benard P, Couvreux F, Lahellec A. 2010. NAM–SCA: Nonhydrostatic anelastic model under segmentally-constant approximation. *Mon. Weather Rev.* **138**: 1957–1974.

